Inorg. Chem. **2006**, *45*, 5691–5702

Ferrocenyl Compound as a Multiresponsive Calcium Chemosensor with Remarkable Fluorescence Properties in CH_3CN

Béatrice Delavaux-Nicot,*,† Jérôme Maynadié,† Dominique Lavabre,‡ and Suzanne Fery-Forgues‡

Laboratoire de Chimie de Coordination du CNRS, UPR 8241, 205, route de Narbonne, F-31077, Toulouse Cedex 04, France, and Laboratoire des Interactions Moléculaires et Réactivité Chimique et Photochimique, UMR 5623 du CNRS, Université Paul Sabatier, 118 route de Narbonne, F-31062, Toulouse Cedex, France

Received March 29, 2006

We have synthesized a novel disubstituted ferrocenyl compound $[Fe(C_5H_4CO(CH{=}CH)_2C_6H_4NEt_2)_2]$ (**3**) that displays a remarkable fluorescence quantum yield (1.1×10^{-1}) in acetonitrile, and we have studied its capacity for calcium detection in depth using both electrochemical and optical techniques in this medium. The results of our NMR analysis reveal that the ligand–calcium interaction is CO-centered and that an uncommon equilibrium occurs between **3** and calcium triflate, involving five species of different stoichiometries. In contrast, our analysis of the UV–vis absorption data indicates that only three species of different stoichiometries are formed when calcium perchlorate is used with **3**. Mass spectrometry measurements provide strong support for the formation of all these different species in solution. In addition, the electrochemical detection of calcium triflate by **3** leads to an irreversible Fe^{II}/Fe^{III} oxidation process with an unusual negative shift (–60 mV) caused by the $^nBu_4NBF_4$ salt effect on the Ca^{2+}–**3** interaction process. Compound **3** can also be an original optical probe to detect calcium perchlorate over a wide range of salt concentration by UV–vis absorption spectroscopy. The most original and intriguing property of compound **3** is that it exhibits an unprecedented "multistep" fluorescence behavior upon addition of this salt.

Introduction

Sensing of ions is an area of increasing research activity[1] because ions play a fundamental role in biology, chemical processes, and environmental pollution. Sensing systems are usually composed of a signaling unit linked to a receptor, so that ion binding is determined by a measurable physical change. An attractive way of achieving a new generation of sensors is to synthesize a molecule that is capable of reporting on the recognition event through a variety of physical responses. This allows thorough information to be obtained by comparing the different physical responses gathered upon addition of an analyte. It also allows the same sensor to be used in various experimental conditions and, possibly, for the detection of different analytes.[2] In this context, the coupling between electrochemical and optical techniques, in particular UV−vis absorption spectroscopy, has recently attracted much attention.[1b,3] An exciting advantage of these systems could be the tuning of the optical properties via oxidation state modulation of the redox center.[4] In this research area, ferrocenyl derivatives are of special interest: (i) from a synthetic standpoint, ferrocene is a very convenient building block for a redox active ligand because it can relatively easily be functionalized and incorporated by many

* To whom correspondence should be addressed. E-mail: delavaux@lcc-toulouse.fr. Fax: 33 (0)5 61 55 30 03.

† Laboratoire de Chimie de Coordination du CNRS.

‡ Université Paul Sabatier.

(1) For some examples, see: (a) Beer, P. D. *Adv. Inorg. Chem.* **1992** *39*, 79−157. (b) Beer, P. D.; Cadman, J. *Coord. Chem. Rev.* **2000**, *205*, 131−155. (c) Delavaux-Nicot, B.; Bigeard, A.; Bousseksou, A.; Donnadieu, B.; Commenges, G. *Inorg. Chem.* **1997**, *36*, 4789−4797 and references therein. (d) Astruc, D.; Daniel, M. C.; Ruiz, J. *Chem. Commun.* **2004**, No. 23, 2637−2649. (e) Ion, A. I.; Ion, J.-C.; Pailleret, A.; Popescu, A.; Saint-Aman, E.; Ungureanu, E.; Siebert, E.; Ziessel, R. *Sens. Actuators* **1999**, *B59*, 118−212. (f) Miyaji, H.; Collinson, S. R.; Prokes, I.; Tucker, J. H. R. *Chem. Commun.* **2003**, No. 1, 64−65. (g) de Silva, A. P.; Gunaratne, H. Q. N.; Gunnlaugsson, T.; Huxley, A. J. M.; McCoy, C. P.; Rademacher, J. T.; Rice, T. E. *Chem. Rev.* **1997**, *97*, 1515−1566. (h) Czarnik, A. *Fluorescent Chemosensors for Ion and Molecule Recognition*; ACS Symposium Series 538; American Chemical Society: Washington, DC, 1993. (i) Tsien, R. Y. In *Methods in Cell Biology*; Taylor, D., Wang, Y.-L, Eds.; Academic Press: London, 1989; Vol. 30, p 127.

(2) Jimenez, D.; Martinez-Manez, R.; Sancenon, F.; Ros-Lis, J. V.; Soto, J.; Benito, A.; Garcia-Breijo, E. *Eur. J. Inorg. Chem.* **2005**, 2393−2403.

(3) (a) Beer, P. D.; Hayes, E. J. *Coord. Chem. Rev.* **2003**, *240*, 167−189. (b) Lopez, J. L.; Tarraga, A.; Espinosa, A.; Velasco, M. D.; Molina, P.; Lloveras, V.; Vidal-Gancedo, J.; Rovira, C.; Veciana, J.; Evans, D. J.; Wurst, K. *Chem.—Eur. J.* **2004**, *10*, 1815−1826.

10.1021/ic060535e CCC: $33.50
Published on Web 06/06/2006

structures, and (ii) its electrochemical and UV−vis spectroscopic properties can be perturbed by the proximity of bound guests. We are especially interested in the fluorescence properties of this kind of derivative. Actually, fluorimetry is presently the optical method that offers the highest sensitivity, and ion recognition by fluorescent sensors has demonstrated the usefulness of this technique. However, ferrocenyl receptors which contain both electroactive and fluorescent signaling units are still rare,[5] probably, because ferrocene derivatives are known to be efficient fluorescence quenchers. [5c,6] Even so, this kind of compound could be the keystone of new families of ion chemosensors, and it has already been announced that the fabrication of these systems and their integration into different supports would certainly lead to novel prototype molecular sensory devices for commercial applications.[1b]

Although the field of research dealing with fluorescent and electrochemical ferrocenyl ion sensors is still in its infancy, a few interesting ligands have already been designed.[5a,7,8,9,10] Let us remark that all the "purely" ferrocenyl receptors[8−10] consist of well-separated three component-systems. They contain one or several ferrocene units, a complexing moiety, and one or several fluorescent moieties, which are connected together by saturated bonds. In the absence of guest, the ferrocene residue acts as a quencher for the fluorescent unit, through the involvement of a photoinduced electron-transfer process. In the presence of an anion, the fluorescence revival observed is the result of the inhibition of this mechanism.

As early as 1999, we first reported a totally different type of ligand, where the ferrocenyl, complexing, and fluorescent moieties belong to the same conjugated π-electron system. To do so, we have investigated the synthesis of electroactive receptors, which combine a ferrocenyl unit and a purely organic fluorescent ion sensor subunit containing an R-amino complexing moiety (−COCH═CHC$_6$H$_4$−*p*R).[5b] Of particular interest is the fact that the monosubstituted compound [(C$_5$H$_5$)Fe(C$_5$H$_4$COCH═CHC$_6$H$_4$NEt$_2$)] (**2**) is not fluorescent, while the disubstituted compound [Fe(C$_5$H$_4$COCH═CHC$_6$H$_4$-NEt$_2$)$_2$] (**1**) (Scheme 1) displays remarkable fluorescence properties and behaves as a new type of optically responsive

Scheme 1. Compounds **1** and **2**

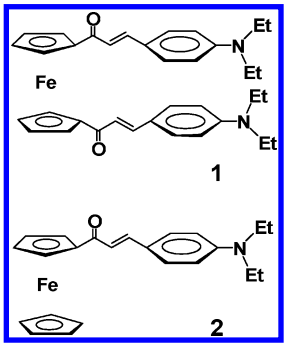

calcium-sensing device in CH$_3$CN.[11] In this compound, the ferrocenyl moiety is far from being a simple fluorescence quencher and acts essentially as an auxochrome.

Since then, other groups have synthesized new conjugated ferrocenyl systems with interesting luminescence properties.[12] A remarkable example is that of Miranda and Molina's team who has recently reported that the addition of 1 equiv of Li^+ to a ferrocene−anthracene-linked dyad remarkably increases its fluorescence intensity (7.3-fold) in an acetonitrile/water (70:30) mixture at pH 5.[12a]

In this promising research field, any accurate or direct comparison concerning the ion detection performances of the few ferrocenyl existing systems is still difficult as numerous parameters involved in the "multisensing phenomenon", such as the medium, the technique considered, or the nature and quantity of the ion, may vary and have to be considered. This is the reason why the introduction focused only on some structural differences that could, in particular, be responsible of the different natures of optical sensing.

In the present study, we are reporting the design of a new ferrocenyl derivative, in which we have retained the disubstituted topology of compound **1** but increased the length of the unsaturated chain. Our goal was 2-fold: first, we wished to obtain another unusual cation sensor with interesting fluorescence and electrochemical properties, and second, we expected to gain a better understanding of the factors that could influence the physical properties in this family. Moreover, we were especially interested in the processes leading to the detection phenomena. Therefore, we have successfully synthesized compound **3** (Scheme 2) and studied two complementary important aspects of its chemistry, which included the following: (1) the capacity of **3** in detecting calcium both by electrochemical and optical techniques in CH$_3$CN and (2) the type of interaction involved with this cation. So, in the following sections, we are describing the preparation and characterization of ligand **3**, and the study of its physicochemical properties without and with calcium salt. In addition to electrochemical and fluorescence measurements, we have also performed thorough ^{1}H NMR and UV−vis investigations concerning the interaction of com-

(4) (a) Harvey, P. D.; Gan, L.; Aubry, C. *Can J. Chem.* **1990**, *68*, 2278−2288. (b) Harvey, P. D.; Gan, L. *Inorg. Chem.* **1991**, *30*, 3239−3241. (c) Cuffe, L.; Hudson, R. D. A.; Gallagher, J. F.; Jennings, S.; McAdam, C. J.; Connelly, R. B. T.; Manning, A. R.; Robinson, B. H.; Simpson, J. *Organometallics* **2005**, *24*, 2051−2060. (d) McGale, E.M.; Robinson, B. H.; Simpson, J.; *Organometallics* **2003**, *22*, 931−939. (e) McAdam, C. J.; Morgan, J. L.; Robinson, B. H.; Simpson, J. *Organometallics* **2003**, *22*, 5126−5136.
(5) (a) Beer, P. D.; Szemes, F.; Balzani, V.; Salà, C. M.; Drew, M. G. B.; Dent, S. W.; Maestri, M. *J. Am. Chem. Soc.* **1997**, *119*, 11864−11875. (b) Delavaux-Nicot, B.; Fery-Forgues, S. *Eur. J. Inorg. Chem.* **1999**, 1821−1825. (c) Fery-Forgues, S.; Delavaux-Nicot, B. *J. Photochem. Photobiol. A* **2000**, *132*, 137−159.
(6) Geoffroy, G. L.; Wrighton, M. S. *Organometallic Photochemistry*; Academic Press: New York, 1979; Chapter 5, pp 230−257.
(7) Beer, P. D.; Graydon, A. R.; Sutton, L. R. *Polyhedron* **1996**, *15*, 2457−2461.
(8) Sancenon, F.; Benito, A.; Hernandez, F. J.; Lloris, J. M.; Martinez-Manez, R.; Pardo, T.; Soto, J. *Eur. J. Inorg. Chem.* **2002**, 866−875.
(9) Oton, F.; Tarraga, A.; Velasco, M. D.; Espinosa, A.; Molina, P. *Chem. Commun.* **2004**, 1658−1659.
(10) Kuo, L.-J.; Liao, J.-H.; Chen, C.-T.; Huang, C.-H.; Chen, C.-H.; Fang, J.-M. *Org. Lett.* **2003**, *5*, 1821−1824.
(11) Maynadié, J.; Delavaux-Nicot, B.; Fery-Forgues, S.; Lavabre, D.; Mathieu, R. *Inorg. Chem.* **2002**, *41*, 5002−5004.
(12) For examples, see: (a) Caballero, A.; Tormos, R.; Espinosa, A.; Velasco, M. D.; Tarraga, A.; Miranda, M. A.; Molina, P. *Organic Lett.* **2004**, 4599−4602. (b) Butler, I. R.; Callabero, A. G.; Kelly, G. A.; Amey, J. R.; Kraemer, T.; Thomas, D. A.; Ligth, M. E.; Gelbrich, T.; Coles, S. J. *Tetrahedron Lett.* **2004**, 467−472.

Scheme 2. Synthetic Route for Compounds **3** and **4**[a]

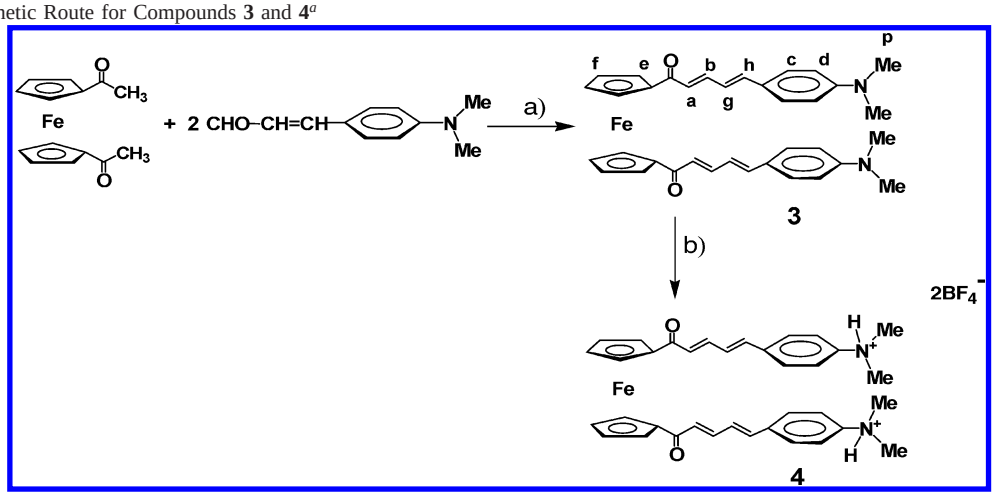

[a] Reagents and conditions: (a) NaOH 1 equiv, ethanol, 20 °C; (b) $HBF_4 \cdot Et_2O$ 2 equiv, CH_3CN, 20 °C.

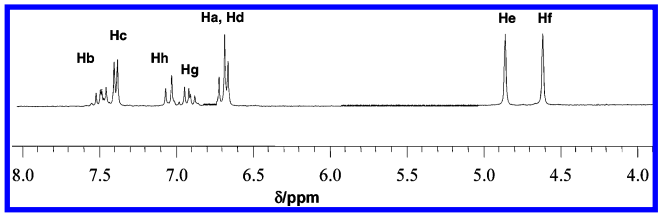

Figure 1. ^1H NMR (400 MHz, CD_3CN) spectra of **3** in the 4−8 ppm range.

pound **3** with calcium to quantify the interaction process that occurs, and we discuss our results. We also present the preparation and characterization of the protonated derivative $[\mathbf{3}H_2][BF_4]_2$ (**4**) which is a key compound in the calcium triflate electrochemical detection process. When useful to make our point, we have compared our present series of data with those previously reported for compounds **1** and **2** and with those of some derivatives of **2**. Finally, in the last section, we highlight the remarkable fluorescence behavior of compound **3** upon calcium addition.

Results and Discussion

Synthesis and Characterization of Compound 3 and of its Protonated Derivative 4. The synthesis of compound **3** was realized by reaction of the 1,1′-diacetylferrocene with 2 equiv of the appropriate aldehyde in basic medium (Scheme 2). The product was isolated in a good yield (65%) as a red-orange powder. Its structure was deduced from spectroscopic NMR data, which also revealed the perfect symmetry of the molecule with the protons of the two branches giving exactly the same signal. The ^1H NMR spectra of **3** in the 4−8 ppm range is provided in Figure 1. 2D NMR experiments at 400 MHz were undertaken in CD_3CN to provide a complete assignment of each signal. The IR spectrum exhibited a ν(C═O) vibration at 1645 cm^{-1}, this low value being the result of the conjugation of this group with the rest of the molecule.[13] The elemental analyses and mass spectra were in agreement with the formula proposed for **3** in Scheme 2 (see Experimental Section).

(13) Silverstein, R. M.; Bassler, G. C.; Morril, T. C. In *Spectrometric Identification of Organic Compounds*, 4th ed.; J. Wiley and Sons: New York, 1981; pp 117−118.

Table 1. ^1H NMR and ^{13}C Shift Variations ($\Delta(\delta)$, ppm) of Selected Groups of Compound **3** upon (a) Protonation and (b) Calcium Addition (2 equiv)[a]

	CHa	CHb	CHc	CHd	CHp	CHe	CHf	CHg	CHh	CO
					(a) **3** + $2H^+$					
^1H	0.19	0.00	0.36	0.93	0.26	0.05	0.07	0.33	0.09	
^{13}C	3.70	−2.33	0.09	9.20	7.62	0.26	0.81	7.66	−4.28	0.04
					(b) **3** + $2Ca^{2+}$					
^1H	−0.12	0.28	−0.14	−0.09	0.00	0.16	0.21	−0.10	0.06	
^{13}C	−2.11	6.11	0.81	−0.21	−0.07	1.26	1.44	−0.67	4.49	2.24

[a] [L] = 5 $\times 10^{-3}$ M; see group labeling in Scheme 2; ^1H NMR {400.13 MHz} in CD_3CN at 293K; (−) upfield shift.

Upon treatment of a CH_3CN solution of compound **3** with $HBF_4 \cdot Et_2O$ in a 1:2 stoichiometry, the solution turned from red to pink, affording the protonated species $[\mathbf{3}H_2][BF_4]_2$ (**4**). Compound **4** was isolated in good yield (68%). Its characterization was fully achieved by ^1H and ^{13}C 2D NMR experiments. In the ^1H NMR spectrum (CD_3CN, 400 MHz), the protonation reaction was confirmed by the appearance of a new signal at 8.95 ppm attributed to the proton of the NH^+ group.[1c,14] The NCH_3 groups appeared at a downfield-shifted position lower than those of **3** (0.26 ppm), which is consistent with the quaternarization of the nitrogen atom. In Table 1a, the variations of the ^1H and ^{13}C NMR shift show that the molecule is totally affected by the protonation of the nitrogen atom.

NMR Study of the 3−Ca^{2+} Interaction. A. Nature of the Interacting Sites. Since we will show in the next section that compound **3** detects calcium salt electrochemically, we have chosen to examine the **3**−Ca^{2+} interaction process responsible for this detection. First, to determine the nature of the interacting site, we recorded the ^1H NMR spectra of compound **3** in CD_3CN in the presence of 2 equiv of calcium salt. Next, to properly ascertain the variations of the shift observed, we have performed 2D NMR experiments.

As we indicated in Table 1b,^1H NMR shift variations were observed along the whole conjugated link, with the strongest shift being associated with the Hb protons. In contrast to the protonation reaction, calcium addition did not induce drastic shifts in the vicinity of the nitrogen atom, and the Hp protons were unaffected. The ^{13}C NMR shift variations

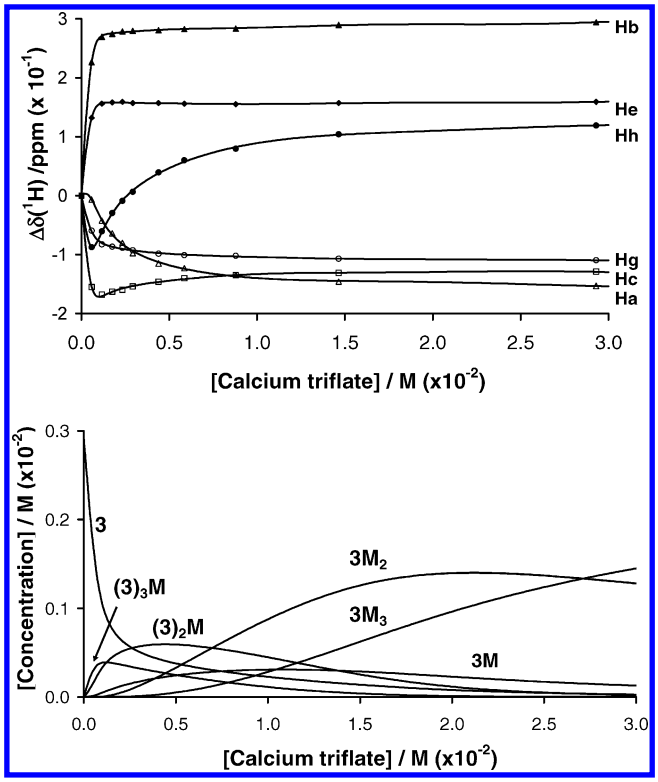

Figure 2. (top) ^{1}H NMR chemical shift variations of the mentioned protons of **3** (2.93×10^{-3} M) vs the $Ca(CF_3SO_3)_2$ concentration in CD_3CN at 293 K. Experimental values (▲, ♦, ●, ○, □, △) and calculated (—) curves obtained by fitting the data. See atom labeling in Scheme 2. (bottom) Concentration of the species formed versus calcium concentration.

indicate that the conformational changes of the molecule were less drastic than for the protonation reaction, the most important variations being obtained for the CHb and CHh groups. The CO groups of **3** were more perturbed upon Ca^{2+} addition than upon protonation. Thus, compound **3** behaved differently upon protonation and calcium addition. In the latter case, the shifts observed suggested that the CO groups were the key points of the interaction. These observations are reminiscent of the NMR behavior of compound **1** and of that of the *N*-alkyl-monosubstituted homologues, upon calcium addition.[11,15]

B. Analysis of the ^{1}H NMR Data and Proposition of a Model for Ca^{2+} Interaction. To get a better insight into the **3**−Ca^{2+} interaction process, the number and stoichiometry of the calcium adducts involved were determined by processing the ^{1}H NMR data acquired at 293 K. Actually, the continuous shifts of the sharp peaks observed during the calcium titration experiments were indicative of the presence of fast equilibriums on the NMR time-scale,[16] and the chemical shift variations of six protons of **3** were successfully plotted versus calcium concentration (Figure 2, dots). Figure 2 clearly illustrates that all these protons are involved in the CO-centered interaction: the whole unsaturated core of the molecule including the Cp rings contributes to the electronic interaction with the cation.

Table 2. Association Constants Related to the Different Formed Species with Ligand **3** and Calcium Triflate in Acetonitrile, Determined by Processing the NMR Data[a]

3M K_1 (M^{-1})	$(\mathbf{3})_2$M K_2 (M^{-1})	**3**M_2 K_3 (M^{-1})	$(\mathbf{3})_3$M K_4 (M^{-1})	**3**M_3 K_5 (M^{-1})
2.07×10^2	6.41×10^3	4.37×10^2	1.11×10^3	4.93×10^1

[a] Values given with ±15% error.

The curves (Figure 2) were then processed according to a global curve-fitting method previously reported,[17,18,19] and the analysis was performed simultaneously for the six protons considered. Complete agreement between theory and experiment could only be obtained by taking into account the existence of five species with different stoichiometries. They are formed by compound **3** with calcium and can be written as: **3**M, $(\mathbf{3})_2$M, **3**M_2, $(\mathbf{3})_3$M, and **3**M_3 (where M is the calcium cation). Their corresponding association constants (K_n) are given in Table 2. In Figure 2 (top), we displayed the ^{1}H NMR experimental data points together with the calculated curves to show the quality of the fit. More precisely, it must be noted that no correct fit (see S2) could be obtained without considering the $(\mathbf{3})_2$M and $(\mathbf{3})_3$M species. Then, taking into account the **3**M_2 and **3**M_3 species allowed the residual error, E_r (see Experimental Section), to be significantly reduced from 2.9×10^{-5}, with 3 species, to 4 $\times 10^{-6}$, with 5 species.

As shown in Figure 2 (bottom), the calculated concentrations of the species formed versus calcium concentration indicate that, while $(\mathbf{3})_2$M and $(\mathbf{3})_3$M are the main species at low concentration, **3**M_2 and **3**M_3 are the major compounds at high calcium concentration. The $(\mathbf{3})_2$M and $(\mathbf{3})_3$M forms present the highest association constants, whereas **3**M_3 has the smallest one. In comparison to the alkyl-monosubstituted homologues under the same conditions, the association constants of the $(\mathbf{3})_n$M species are higher by 1 or 2 orders of magnitude, which could be explained by the involvement of the two arms of the molecule in the association processes.

The formation of substoichiometric compounds of the L_nM type where $n = 2$ or 3 is very likely, as the Ca^{2+} may interact with six to nine donor atoms in the case of organic ligands exhibiting the −C═C−C═O linkage, according to the Cambridge Crystallographic Data Centre database. We have previously developed this point in refs 15 and 19. The formation of the **3**M_3 species may be surprising. However, the triflate ion may also interact with the Ca^{2+} ion, for example through its O and F atoms, thereby increasing the number and nature of possible donor atoms and existing

(14) Silverstein, R. M.; Bassler, G. C.; Morril, T. C. In *Spectrometric Identification of Organic Compounds*, 4th ed.; J. Wiley and Sons: New York, 1981; Chapter 3, p 198.
(15) Maynadié, J.; Delavaux-Nicot, B.; Lavabre, D.; Donnadieu, B.; Daran, J. C.; Sournia-Saquet, A. *Inorg. Chem.* **2004**, *43*, 2064−2077.
(16) (a) Hynes, M. J. *J. Chem. Soc., Dalton Trans.* **1993**, 311−312. (b) Fielding, L. *Tetrahedron* **2000**, *56*, 6151−6170.
(17) Marcotte, N.; Fery-Forgues, S.; Lavabre, D.; Marguet, S.; Pivovarenko, V. G. *J. Phys. Chem.* **1999**, *A103*, 3163−3170.
(18) Fery-Forgues, S.; Lavabre, D.; Rochal, D. *New J. Chem.* **1998**, *22*, 1531−1538.
(19) Delavaux-Nicot, B.; Maynadié, J.; Lavabre, D.; Lepetit, C.; Donnadieu, B. *Eur. J. Inorg. Chem.* **2005**, 2493−2505.

Table 3. Assigment of the Main Peaks Obtained by Mass Spectrometry Using the Positive FAB and the ESI-MS* Techniques for Compound **3** (5×10^{-3} M) in the Presence of Calcium[a]

	$[\mathbf{3}MX]^+$	$[(\mathbf{3})_2M]^{2+}$*	$[(\mathbf{3})_2MX]^+$	$[(\mathbf{3})_3M]^{2+}$*	$[(\mathbf{3})_3MX]^{+}$*	$[\mathbf{3}M_2X_3]^+$	$[\mathbf{3}M_3X_5]^+$
$Ca(CF_3SO_3)_2$	773	604.5	1358	896.5		1111.0	1449.0
$Ca(ClO_4)_2$	723	604.5	1307	896.5	1893		

[a] M = Ca^{2+}; X = $CF_3SO_3^-$ or ClO_4^-.

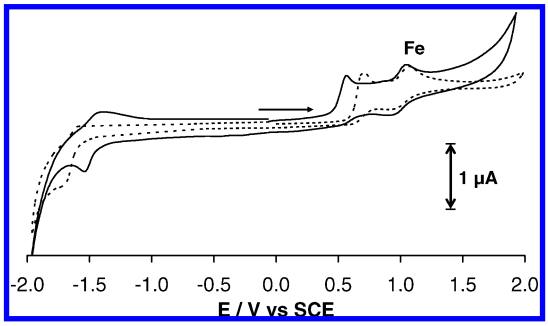

Figure 3. Cyclic voltammograms of compounds **1** (- - -) and **3** (—). Experimental conditions: Pt electrode (1 mm diameter) in 0.1 M solution of $^nBu_4NBF_4$ in CH_3CN, scan rate 100 mV s^{-1}, ligand concentration 10^{-3} M, reference electrode SCE.

interactions.[20] This hypothesis could help in the understanding of the formation of the LM_m species.

Thus, for the concentration used, several species compete in solution. It can be noted that, in the reported equilibriums, weak intermolecular interactions[21] (for example with adjacent phenyl groups) or electrostatic interactions, rather than classical complexation reactions, may also be considered.

In addition, samples of **3** (5×10^{-3} M) containing 0.5, 1, and 2 equiv of calcium salt were prepared as for the NMR measurements, and their mass spectra were recorded. The positive FAB technique using an MNBA matrix and the ESI-MS revealed all the peaks expected for the five compounds (Table 3), providing thus strong support for their formation in solution.

Electrochemical Studies. A. Characterization of Compound 3 and In Situ Formation of 4. The electrochemical properties of compounds **3** and **4** have been investigated in CH_3CN. A typical voltammogram of compound **3** is shown in Figure 3. In oxidation, the wave observed in cyclic voltammograms (CV) at $E_{p_a} \cong 1.12$ V is from the oxidation of the ferrocene moiety and corresponds to a quasi-reversible process. The first complex irreversible oxidation process of compound **3**, whose $E_{1/2}$ value is 0.56 V, may be attributed to the oxidation of the organic amine moiety.[15,22] This potential lies in the range of values reported for the oxidation of some aza ferrocenyl compounds.[23] This oxidation process is reminiscent of the electrochemical behavior of the organic compound $CO(CH{=}CHC_6H_4NEt_2)_2$ under the same conditions.[15] As shown in Figure 3, the electrochemical characteristics of **3** are very similar to those of compound **1**. However, insertion of a supplementary −C═C− unit after the CO group of **1** induces an increase of the electron density in the organic moiety and, consequently, a decrease of its oxidation potential of 90 mV. The same kind of observation was made when comparing the monosubstituted derivative $[(C_5H_5)Fe(C_5H_4CO(CH{=}CH)_2C_6H_4NMe_2)]$ with compound **2**.[15] In reduction, the single wave observed at $E_{p_a} = -1.80$ V for compound **3** was attributed to a reduction process mainly located on the CO function.

Upon addition of 2 equiv of $HBF_4{\cdot}Et_2O$, the electrochemical solution of compound **3** in CH_3CN turned from red to red-pink. A cathodic shift of − 60 mV was induced for the Fe^{II}/Fe^{III} couple. This oxidation process became irreversible, and a passivation phenomenon caused by a nonconducting deposit on the electrode prevented determination of its $E_{1/2}$ value by linear voltammetry. It is noteworthy that this cathodic variation is weaker than that observed for compound **1** (−120 mV) under the same conditions. In parallel, the complex wave attributed to the oxidation of the organic moiety disappeared, and the wave corresponding to the NH^+ reduction process appeared at −0.35 V. The final intensity of these different processes is in agreement with the formation of the protonated species, **4**. Direct measurements of the electrochemical characteristics of compound **4** were not easy: under these conditions, a partial deprotonation rapidly occurred and prevented accurate data from being obtained.

B. From Calcium−Ligand Interaction to Electrochemical Detection. To investigate the capacity of compound **3** as a calcium electrochemical sensor, 2 equiv of $Ca(CF_3SO_3)_2$ was added to a solution of **3** under the same electrochemical conditions. A broad ill-defined process indicated that the CO reduction process was strongly perturbed, and a new irreversible reduction process appeared around −0.35 V. In oxidation, electrochemical characteristics close to those induced by the in situ protonation of compound **3** were obtained (see Figure 4). Further addition of salt (up to 10 equiv) had no significant effect.

Thus it seems that the interaction with calcium leads to the same electrochemical response as protonation. Taking into account the outcome of the electrochemical detection of calcium by the monosubstituted homologues, we had suspected a peculiar role of the electrolyte. Therefore, the calcium−ligand interaction process was re-examined in the presence of the Et_4NBF_4 supporting electrolyte, following

(20) (a) Lawrance, G. A. *Chem. Rev.* **1986**, *86*, 17−33. (b) Frankland, A. D.; Hitchcok, P. B.; Lappert, M. F.; Lawless, G. A. *J. Chem. Soc., Chem. Commun.* **1994**, 2435−2436. (c) Onoda, A.; Yamada, Y.; Doi, M.; Okamura, T.; Ueyama, N. *Inorg. Chem.* **2001**, *40*, 516−521.

(21) (a) Gokel, G. W.; De Wall, S. L.; Meadous, E. S. *Eur. J. Org. Chem.* **2000**, 2967−2978. (b) Meadous, E. S.; De Wall, S. L.; Barbour, L. J.; Gokel, G. W. *J. Am. Chem. Soc.* **2001**, *123*, 3092−3107. (c) Ma, J. C.; Dougherty, D. A. *Chem. Rev.* **1997**, 13033−1324. (d) Futterer, T.; Merz, A.; Lex, J. *Angew. Chem., Int. Ed. Engl.* **1997**, *36*, 611−613.

(22) (a) Spescha, M.; Duffy, N. W.; Robinson, B. H.; Simpson, J. *Organometallics* **1994**, *13*, 4895−4904. (b) Duffy, N. W.; Harper, J.; Ramani, P.; Ranatunge-Bandarage, R.; Robinson, B. H.; Simpson, J. *J. Organomet. Chem.* **1998**, *564*, 125−131.

(23) Andrews, M. P.; Blackburn, C.; McAleer, J. F.; Patel, V. D. *J. Chem. Soc., Chem. Commun.* **1987**, 1122−1124.

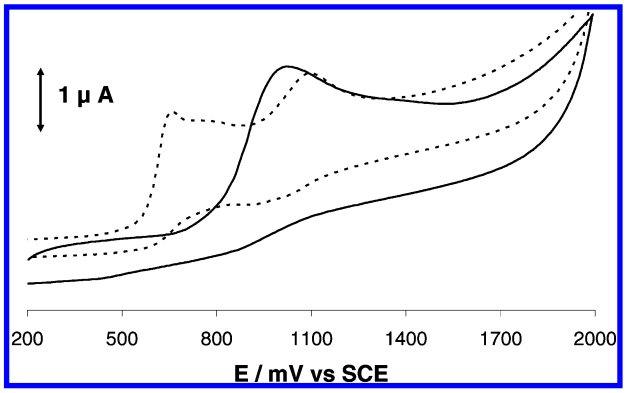

Figure 4. Cyclic voltammograms of compound **3** in oxidation before (- - -) and after (—) addition of 2 equiv of calcium triflate. Experimental conditions: Pt electrode (1 mm diameter) in 0.1 M solution of $^{n}Bu_4NBF_4$ in CH_3CN, scan rate 100 mV s^{-1}, ligand concentration 10^{-3} M, reference electrode SCE.

the procedure detailed in ref 15. It was verified that the calcium−ligand **3** interaction process was stable over 48 h in the absence of the supporting electrolyte and that ligand **3** alone was insensitive to the presence of this ammonium salt. In contrast, the preparation of a 1:2:2 mixture of **3**/Ca^{2+}/Et_4NBF_4 in CD_3CN clearly afforded complex **4**. Therefore, it appears that the Ca^{2+}/BF_4^- couple was responsible for the formation of the protonated species, **4**, in the presence of a small amount of water provided by the electrochemical or NMR medium. The protonation that follows the Ca^{2+} interaction process with **3** allows indirect calcium detection. Such a mechanism has already been encountered for the monosubstituted compound **2** and its derivatives.[15,19]

Actually, the apparent cathodic shift of the iron potential ($\Delta E_{p_a} = -60$ mV) observed for ligand **3** upon Ca^{2+} addition corresponds to the shift induced by ligand protonation. Thus, the observed ΔE_{p_a} of the Fe^{II}/Fe^{III} couple represents the difference of the oxidation potential between the protonated form, $[Fe^{II}N_2H_2^{2+}]$ **4**, and its neutral form, $[Fe^{II}N_2]$ **3**. In compound **3**, the first oxidation potential of the molecule, attributed to the organic amino moiety, precedes the iron oxidation potential. Consequently, the oxidation of **3** first leads to the formation of a cationic radical species probably $[Fe^{II}N_2^{2+\bullet}]$, whose E_{p_a}(Fe) value (1.11 V) is higher than that observed for its corresponding $[Fe^{II}N_2H_2^{2+}]$ protonated form (1.05 V). The calculated ΔE_{p_a} is negative, and the shift observed is cathodic.

So the "unexpected cathodic shift" noticed for the iron couple upon cation addition is connected with the uncommon nature of molecule **3**. In contrast, for classical electrochemical ferrocenyl sensors whose first oxidation potential is from the iron couple in the protonated and neutral forms, a positive shift is observed upon cation addition.[1b]

In our comparison of the electrochemical behaviors of compounds **3** and **1** upon calcium addition, two main differences appear: first, increasing the distance between the redox center and the amino site decreases the ΔE_{p_a} value of the Fe oxidation process from −120 to −60 mV. For ligand **3**, the electronic communication through the conjugated link is lower than in **1**, which is in agreement with the literature data.[24] Another main difference between ligands **1** and **3** is that the Fe^{II}/Fe^{III} oxidation process becomes clearly irreversible for ligand **3**.

The complete electrochemical study on compounds **3** and **4** allows us to strengthen our explanation for the intriguing and uncommon cathodic potential shift observed upon cation addition. It also suggests us that the singular behavior of compound **3** upon cation addition is of the same nature as that previously encountered with the first disubstituted compound, **1**, which still needed to be elucidated.[11]

It should be added that the electrochemical behavior of compound **3** was also evaluated toward other cations. With Li^+, Na^+, and K^+, electrochemical detection was inefficient, probably because weak associations were involved. The copper and magnesium salts resulted in unclear electrochemical detection and were not studied further. Considering these results and the fact that compound **3** presents an optimal response with calcium, we have chosen to use this salt throughout this work.

Optical Detection of Calcium by Ligand 3. A. Study by UV−vis Absorption Spectroscopy. As mentioned in the Introduction, few ferrocenyl compounds have been investigated for their ability to detect ions by both electrochemical and optical methods.

The optical detection capabilities of ligand **3** toward calcium were evaluated to give further insight into this interaction process under new experimental conditions. UV−vis absorption spectroscopy experiments were performed in CH_3CN. The absorption properties of compound **3** were first determined. At a 2.7×10^{-5} M concentration in acetonitrile, this compound gave an orange solution. The UV−vis absorption spectrum exhibited an intense long-wavelength band at $\lambda_{max} = 420$ nm with a molecular absorption coefficient, ϵ_{420}, of 35 100 L mol^{-1} cm^{-1}. This band was attributed to a charge-transfer (CT) transition resulting from the displacement of the electron density from the donor amino group toward the acceptor carbonyl group.[5b] It was only slightly red-shifted with respect to the CT band of compound **1** (416 nm, $\epsilon_{416} = 44300$ L mol^{-1} cm^{-1}), but it was significantly wider (full width at half-maximum = 5580 and 4650 cm^{-1} for **3** and **1**, respectively). When compared to **1**, the absorption spectrum also displayed a new weak band peaking around 296 nm. These features can be explained by the extension of the conjugated system resulting from the presence of an additional ethylenic unit.[25]

Our aim, in this case, was to explore a wide range of concentration in calcium, which means that a high metal-to-ligand ratio should be attained. In these conditions, the use of calcium triflate did not allow accurate determination of the binding constants, probably because of a side reaction that occurs. Actually, working with the monosubstituted compounds, we have recently shown that the use of the $Ca(CF_3SO_3)_2$ salt at high concentration ($> 5 \times 10^{-3}$ M) may lead to total protonation of the chemosensor (10^{-5} M),

(24) Plenio, H.; Yang, J.; Diodone, R.; Heinze, J. *Inorg. Chem.* **1994**, *33*, 4098−4104.
(25) Kawamata, J.; Akiba, M.; Inagaki, Y. *Jpn. J. Appl. Phys.* **2003**, *42*, L17−L19.

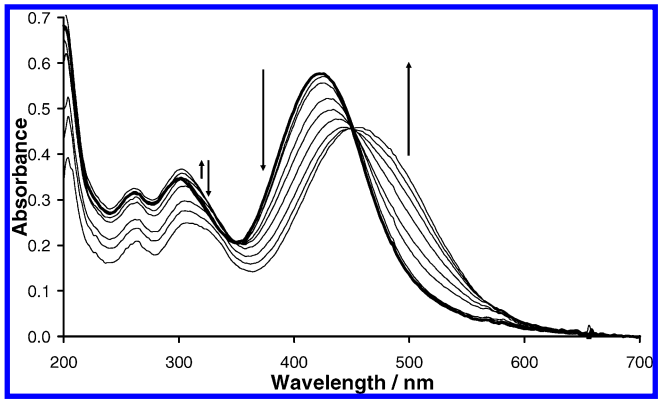

Figure 5. Absorption spectra of compound **3** (1.66×10^{-5} M) in acetonitrile before (−) and after the addition of calcium perchlorate. $Ca(ClO_4)_2 \cdot 4H_2O$ from top to bottom at 418 nm: 0, 7.5×10^{-6}, 5×10^{-5}, 2.5×10^{-3}, 1×10^{-2}, 2.5×10^{-2}, 5×10^{-2}, 7.5×10^{-2}, and 1.0×10^{-1} M.

whereas this phenomenon was not detected using the perchlorate salt.[26] This is the reason why we cannot propose a model with the triflate salt under UV−vis conditions with compound **3**.

Consequently, the use of calcium perchlorate was preferred, this salt being classically used for this type of spectroscopic study. The addition of calcium perchlorate to a solution of **3** led to a reddening of the solution. The intensity of the CT band regularly decreased, whereas the λ_{max} moved to 456 nm (Figure 5), with the formation of a quasi-isosbestic point. The appearance of the band at long wavelengths can be assigned to the interaction of the carbonyl groups with the cation.[11,27]

As for the NMR experiments, one of the aim of the UV−vis absorption study was to determine the number of species involved into the Ca^{2+}−ligand interaction process in these new conditions. To do so, the absorbance variation was analyzed versus cation concentration. Absorbance was recorded at six different wavelengths chosen to obtain maximum information, and the absorption spectroscopic data were processed according to the global curve-fitting method described elsewhere (Figure 6 top).[17,18] Among the different models investigated, good fits were obtained by taking into account the existence of only three species of different stoichiometries: **3**M, $(\mathbf{3})_2$M, and $(\mathbf{3})_3$M. The corresponding association constants were 1.07×10^3, 6.40×10^6, and 3.82×10^6 M^{-1}, respectively (values given with a ±15% error), pointing out the stability of the substoichiometric compounds. Calculated concentrations of the species versus cation concentration are presented in Figure 6 (bottom).

In addition to these titration experiments, mass spectrometry measurements were performed with calcium perchlorate and ligand **3** under the same experimental conditions as in a previous section, and they revealed all the peaks expected for the three species (see Table 3).Unfortunately, it was not possible to obtain any X-ray structures for one of these adducts.

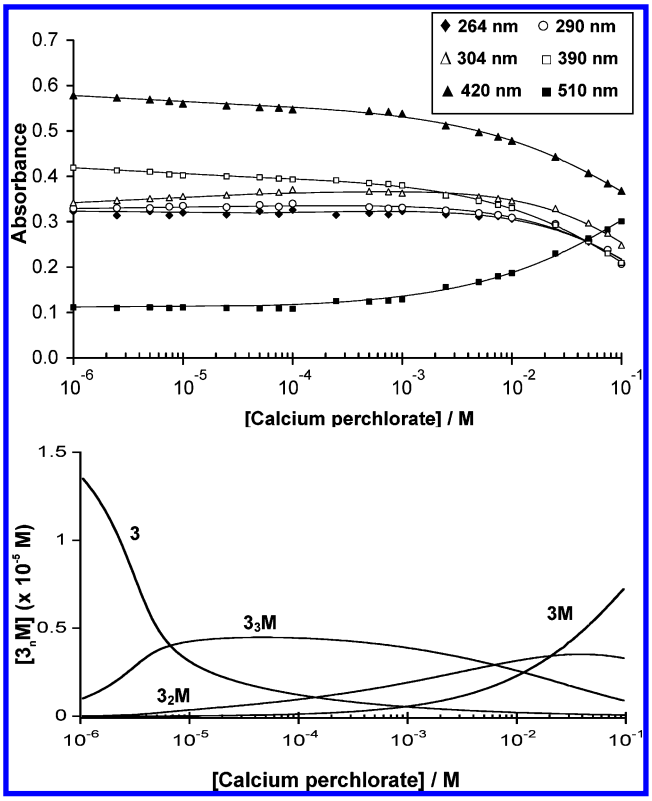

Figure 6. Processing of the UV−vis absorption data for compound **3** (1.66×10^{-5} M) in the presence of calcium perchlorate in CH_3CN. (top) Absorbance vs calcium concentration at different wavelengths in nanometers. The points are experimental and the curves (lines) were calculated by fitting the data. (bottom) Corresponding calculated concentrations of the different species.

However, according to the model proposed, it can be calculated that for a ligand concentration of 1×10^{-3} M and a calcium concentration of around 3.4×10^{-4} M, the formation of the $(\mathbf{3})_3$M species is favored with respect to that of the $(\mathbf{3})_2$M species, while the **3**M species should be in minor proportion. Such a mixture was prepared and directly analyzed by electrospray mass technique. Actually, the spectra clearly displayed peaks which can be attributed to the $(\mathbf{3})_3$M and $(\mathbf{3})_2$M species as their $(\mathbf{3})_2Ca^{2+}$ and $(\mathbf{3})_3Ca(ClO_4)^+$ forms. The calculated and experimental spectra of the $(\mathbf{3})_3Ca^{2+}$ cation were in perfect agreement (see Supporting Information S1). Moreover, although a small peak situated at 312 could be attributed to the $\mathbf{3}M^{2+}$ species, no $\mathbf{3}M_n$ species were identified. One possible formula for the $(\mathbf{3})_3$M compound is the coordination of the same calcium atom to six carbonyl groups belonging to three different ligands. Theoretical investigations performed with compound **1** show that this hypothesis is conceivable.[28]

When comparing the results obtained by UV−vis absorption spectroscopy using calcium perchlorate with those of the NMR analysis carried out with calcium triflate, it appears that the number of species involved in the ligand−calcium interaction and the value of their association constants are markedly different. This is probably caused by the nature of the symmetrical ClO_4^- anion which allows fewer associations with calcium than the large $CF_3SO_3^-$ anion, bearing more

(26) Maynadié, J.; Delavaux-Nicot, B.; Lavabre, D.; Fery-Forgues, S. *J. Organomet. Chem.* **2006**, 1101−1109.
(27) Ukai, T.; Kawazura, H.; Ishii, Y.; Bonnet, J. J.; Ibers, J. A. *J. Organomet. Chem.* **1974**, *65*, 253−266.
(28) Delavaux-Nicot, B.; Lepetit, C. Unpublished results.

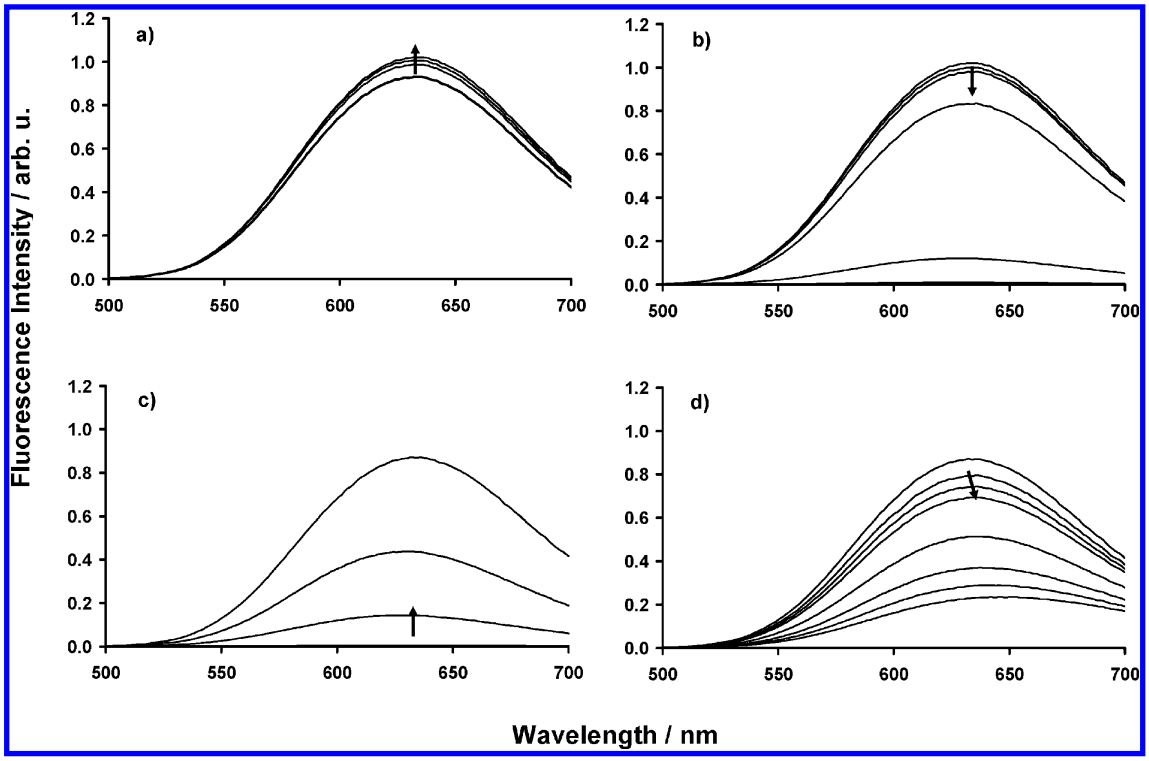

Figure 7. Fluorescence spectra of ligand **3** (1.68×10^{-6} M) in acetonitrile before and after addition of calcium perchlorate ($\lambda_{ex} = 452$ nm). $Ca(ClO_4)_2 \cdot 4H_2O$: (a) from bottom to top 0, 1.0×10^{-6}, 2.5×10^{-6}, and 7.5×10^{-6} M; (b) from top to bottom 7.5×10^{-6}, 1.0×10^{-5}, 5.0×10^{-5}, 1.0×10^{-4}, 2.9×10^{-4}, and 5.0×10^{-4} M; (c) from bottom to top 5×10^{-4}, 7.5×10^{-4}, 1.0×10^{-3}, and 2.5×10^{-3} M; (d) from top to bottom 2.5×10^{-3}, 5.0×10^{-3}, 7.5×10^{-3}, 1.0×10^{-2}, 2.5×10^{-2}, 5.0×10^{-2}, 7.5×10^{-2}, and 10^{-1} M.

donating heteroatoms, as previously evoked. As we will show it in a future paper, this seems to be a general rule when using other disubstituted ligands of this family. However, an NMR study repeated with calcium perchlorate showed that the same interacting sites of ligand **3** were involved, regardless of the anion used.

B. An Intriguing Fluorescence Behavior upon Calcium Addition. As already mentioned, very few ferrocenyl derivatives have a satisfying fluorescence efficiency. Compound **3** was designed to possess this original property, and possibly, to act as a fluorescent probe for cation detection.

In the absence of salt, the emission spectrum of **3** in acetonitrile displayed an intense unresolved emission band peaking at 628 nm, independent of the excitation wavelength. It can be noted that the emission spectrum of **3** was red-shifted by 68 nm when compared to that of compound **1**. This red shift can be assigned to the lengthening of the conjugated π-electron system and may be of interest for biological purposes.[29] In CH_3CN, the quantum yield was up to 1.1×10^{-1} (i.e., slightly higher than that of compound **1**, 7.7×10^{-2}). This result was rather surprising. In fact, a decrease of the quantum yield could have been expected because the insertion of a C═C unit into the basic structure of compound **1** may generate new rotation and vibration modes, thus increasing the possible pathways for nonradiative deactivation. It must also be underlined that the fluorescence emission is not systematic for other symmetrical disubstituted compounds of this family, as will be described in a future study.

Compound **3** was studied in different solvents. Both absorption and emission spectra were shifted to the red when the solvent polarity increased. This behavior is reminiscent of that of compound **1** and indicates that the dipole moment of **3** also increases in the excited state. However, the magnitude of the solvatochromic effect observed here must be pointed out. For instance, the emission spectrum of **3** was shifted from 536 to 630 nm when passing from dioxane to acetonitrile, while the absorption spectrum was only shifted by 4 nm. This leads to exceptionally high Stokes shifts,[30] reaching more than 8000 cm^{-1} in acetonitrile. This effect is generally correlated to a large change in geometry or to a strong variation of the charges within the molecule upon excitation, leading to the subsequent modification of the solvent shell around the excited chromophore.[30] In addition, in a protic solvent, for example, ethanol, the absorption and emission spectra were situated at longer wavelengths ($\lambda_{abs} = 434$ nm, $\lambda_{em} = 662$ nm) than in aprotic solvents of similar polarity. This reveals the formation of a hydrogen bond between the solvent molecules and the ligand carbonyl group.[31]

In the presence of calcium perchlorate, compound **3** (1.68×10^{-6} M) was excited at 452 nm to minimize the effect of absorption variations. Figure 7 shows that an intriguing

(29) Burdette, S. C.; Walkup, G. K.; Spingler, B.; Tsien, R. Y.; Lippard, S. J. *J. Am. Chem. Soc.* **2001**, *123*, 7831−7841. (b) Czarnik, A. W. *Chem. Biol.* **1995**, *2*, 423−428.

(30) Suppan, P.; Ghoneim, N. In *Solvatochromism*; The Royal Society of Chemistry: Cambridge, U.K., 1997; pp 17−18.

(31) Marcotte, N.; Fery-Forgues, S. *Perkin Trans. 2* **2000**, No. 8, 1711−1716.

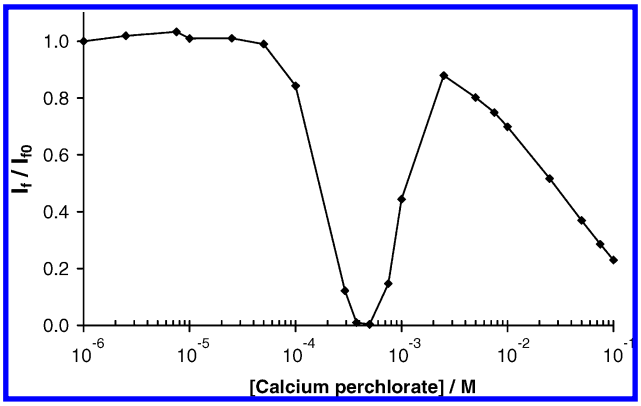

Figure 8. Ligand **3** (1.68×10^{-6} M), variation of the fluorescence intensity ratio at 630 nm versus calcium concentration in CH_3CN ($\lambda_{ex} = 452$ nm).

"multistep behavior" was observed. First, the emission intensity was very slightly increased until the Ca^{2+} concentration reached 7.5×10^{-6} M, then it decreased steeply without any shift in wavelength (630 nm) until fluorescence was totally quenched at a 5×10^{-4} M salt concentration. The addition of salt until a concentration of 2.5×10^{-3} M led to a revival of fluorescence, the band now being centered at 636 nm. Further stepwise addition of salt induced a new decrease of the emission intensity, accompanied by a subsequent red shift (12 nm) of the emission maximum. Figure 8 illustrates this intriguing behavior at $\lambda_{em} = 630$ nm.

The excitation spectrum was recorded for the free ligand and in the presence of six different salt concentrations. For the free ligand, the excitation maximum was situated at 424 nm, independent of the emission wavelength at which the spectrum was recorded. This indicates that fluorescence comes from only one species, as could be expected. It can be noted that the excitation maximum was slightly red-shifted by 4 nm with respect to the absorption maximum. This could be a result of the free dye taking different conformations in solution, some of them being nonemissive.[30] For calcium concentrations of less than 2.5×10^{-3} M, the excitation spectrum was unchanged. For very high concentrations (1×10^{-1} M), the excitation spectrum moved to long wavelengths. The excitation spectrum peaked at 430 nm when emission was recorded at 648 nm and at 438 nm when emission was set at 700 nm. Conversely, the emission spectrum passed from 648 to 694 nm when excitation was performed at 452 and 500 nm, respectively. These observations indicate that at least two species responsible for fluorescence coexist in solution, at high salt concentrations.

These results give a comprehensive view of the fluorescence behavior of compound **3** in the presence of calcium. It seems clear that, in low salt concentrations, the emissive species is the free ligand. The first collapse of the fluorescence intensity can be attributed to the fact that the free species becomes scarce because of the formation of the complexes. This implies that the first complexes formed (most likely, the $(\mathbf{3})_3$M and, maybe, the $(\mathbf{3})_2$M species) are not emissive. Then, when the fluorescence revival is observed for calcium concentrations between 5×10^{-4} and 2.3×10^{-3} M, it is accompanied by a shift in the position of the emission spectrum, even if the excitation spectrum was unchanged. The emitting species is now different from the free ligand. With the complexity of the system, it is very difficult to identify this emitting species, although it is tempting to think that the fluorescence comes from the **3**M complex, which forms in a large proportion at high calcium concentrations. An interesting hypothesis would be that the fluorescence revival observed is the result of the rigidification of the ligand in the complex formed. A possible explanation for the final collapse of fluorescence intensity (calcium concentration $> 2.3 \times 10^{-3}$ M) is that it comes from the presence of water in solution, each calcium perchlorate molecule being associated with four molecules of water. The emissive complex could coexist in solution with its hydrated form, the latter being poorly fluorescent. For the sake of comparison, the emission spectrum of **3** (1.44×10^{-6} M) in the absence of calcium was recorded upon the addition of water. When the water concentration was higher than 5.0×10^{-3} M, a regular decrease of intensity, together with a red-shift, were observed. For instance, with 5×10^{-1} M water, the fluorescence intensity was reduced by 45%, and the spectrum was shifted by 18 nm. This indicates that the excited state of **3** is affected by the presence of water. However it can be noted that quite high concentrations of water are necessary for a quenching effect to be noticeable. It must be outlined that the sensitivity to the presence of water only concerns the excited state of **3**. It was not detected with the ground state of **3**. For this reason, a good fit of the UV−vis absorption data could be attained without taking into account the involvement of water in the complexation process.

To have a better insight into this strange phenomenon, complementary experiments were performed. The concentration of each species present in solution was calculated, taking into account the ligand and calcium concentrations used in fluorescence experiments. To do so, the curve-fitting model obtained when processing the UV−vis data was used, so the calculated concentrations refer to the species in their ground states. This approach confirms that the different species appear in the same order as for UV−vis absorption experiments. It was also noted that, at the point of maximum quenching effect, the concentrations of the three species **3**, $\mathbf{3}_3$M, and $\mathbf{3}_2$M are almost identical (S4). Let us assume that the adducts $\mathbf{3}_3$M and $\mathbf{3}_2$M are not fluorescent and that the only fluorescent species in solution is the free ligand, since the concentration of the latter is divided by about three when compared to its initial concentration, the fluorescence intensity at this point should be one-third of the initial fluorescence intensity. However, it is far lower, which suggests that a more complex phenomenon, for example an intermolecular quenching reaction, occurs in the excited state. It is noteworthy that, according to this model, the subsequent enhancement of fluorescence intensity corresponds to the formation of the LM species.

The titration experiment was repeated with two different concentrations of the ligand (i.e., 7.4×10^{-7} and 3.9×10^{-7} M). The minima of the fluorescence titration curves were then shifted, and their shapes were different from that of the curve previously obtained with a ligand concentration of 1.68×10^{-6} M. In particular, no total fluorescence

Scheme 3. Species Involved in the Equilibria Observed[a]

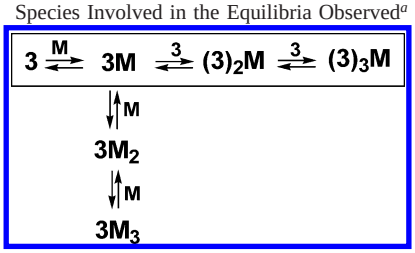

[a] All the species are detected under NMR conditions with the $Ca(CF_3SO_3)_2$ salt. Only the species written horizontally are detected under UV−vis conditions with the $Ca(ClO_4)_2$ salt. As mentioned in the text and developed in refs 15 and 19, one stoichiometry may correspond to several formulas.

quenching was observed. This can be explained by the fact that the respective concentrations of all the species present in solution varies depending on the initial concentration of free ligand. Consequently, for a given calcium concentration, the signal intensity can be somewhat different, according to the initial ligand concentration.

Because compound **3** displays the same fluorescence intensity in the presence of two different salt concentrations, this compound does not appear as a convenient fluorescence calcium sensor. However, the originality of its fluorescence behavior in the presence of calcium perchlorate must be underlined. In this respect, compound **3** totally differs from its disubstituted homologue **1**, for which a more classical behavior will soon be presented.[32] To our knowledge, such an emission behavior has never been reported previously for organic chalcone derivatives in the presence of salts and is also totally unprecedented for ferrocene compounds.

Concluding Remarks

We have designed compound **3** according to a "three-component conjugated concept" and have shown that this new ligand is easy to prepare and allows calcium detection by both electrochemistry and UV−vis absorption techniques. This multiresponsive ferrocene receptor binds a calcium guest via a complex process involving its CO functions and its whole unsaturated core. In addition, we have proposed the quantification of the ligand−cation interaction process for calcium triflate under NMR conditions and for calcium perchlorate under UV−vis absorption spectroscopy conditions. In each case, for the ligand−calcium equilibrium considered, several species were involved as summarized in Scheme 3. Furthermore, their existence was supported by mass spectrometry, and we have successfully determined the values of their association constants. The use of two different calcium salts certainly emphasized the role of the anion, which can determine the number and nature of the formed adducts. However, this phenomenon may also result from the different concentrations and time scales employed in the different techniques.[33] At this point, we would like to underline the fact that the subject of ligand−ion interaction has seldom been addressed in previous publications dealing with electrochemical ferrocenyl ion sensors. In regard to the electrochemical properties, a noticeable $E_{1/2}$ shift of the Fe^{II}/Fe^{III} couple was observed upon calcium triflate addition, but this couple became irreversible. Indeed, we have rationalized this efficient calcium sensing in terms of successive calcium interaction and protonation reactions. Finally, in contrast to similar compounds reported in the literature, our new disubstituted ligand **3** presents good fluorescence properties with an interesting quantum yield and a spectacular solvatochromic effect. To our knowledge, this is the first example of a ferrocene-based sensor whose emission response shows a "multistep" behavior in the presence of a cation. These peculiar properties are directly linked to the insertion of an additional −CH═CH− unit into the molecular framework of **1**. Surprisingly, under our experimental conditions, while this insertion only induces modest changes in the electrochemical calcium detection, the fluorescence calcium sensing is considerably modified and of an unprecedented and intriguing nature. To our knowledge, this optical behavior has never been observed with commercially available calcium fluorescent sensors, which are, in fact, based on organic derivatives generally used under physiological conditions.[1i,34]

In conclusion, we have demonstrated that the conjugated purely ferrocenyl fluorescent compound **3** shows an original behavior in both electrochemical and optical calcium sensing. Our results support clearly the premise that other interesting properties will also be obtained with simple but efficient modifications of the basic framework of **1**. In this respect, we are studying new structures, bearing for example crown-ether groups instead of terminating *N*-alkyl groups, to improve sensitivity of the system. The possibility of developing molecules that can be used in aqueous media is also under consideration.

From a general point of view, this study suggests that the development of this kind of receptors opens wide perspectives in the design of a novel generation of attractive multiresponsive molecules with surprising properties.

Experimental Section

Materials. Toluene, THF, and ether were distilled over sodium/benzophenone; pentane, dichloromethane, and CH_3CN (pure SDS) were distilled over CaH_2 and stored under argon. Analytical grade EtOH (purex SDS) was simply degassed. $Fe(C_5H_4COMe)_2$ (95%), $CHOCH{=}CHC_6H_5NMe_2$ (98%), and HBF_4 54% in Et_2O were from Aldrich. Calcium salts, $Ca(CF_3SO_3)_2$ (96%) and $Ca(ClO_4)_2{\cdot}4H_2O$ (99%), were from Strem and Aldrich, respectively. ***Caution:*** *Perchlorate salts are hazardous because of the possibility of explosion!*

General Instrumentation and Procedures. All syntheses were performed under a nitrogen atmosphere using standard Schlenk tube techniques. The solutions of compounds **3** and **4** were light-protected before each measurement. IR spectra were recorded on a Perkin-Elmer GX FT-IR spectrophotometer. Samples were run as KBr pellets. Elemental analyses were carried out on a Perkin-Elmer 2400 B analyzer at the L.C.C. Microanalytical Laboratory in Toulouse. Mass spectra were obtained at the Service Commun de

(32) Delavaux-Nicot, B.; Maynadié, J. Unpublished results.
(33) Beer, P. D.; Blackburn, H. S. C.; McAleer, J. F. *J. Organomet. Chem.* **1988**, *350*, C15−C19. (b) Beer, P. D.; Keefe, A. D.; Blackburn, H. S. C.; McAleer, J. F. *J. Chem. Soc., Dalton Trans.* **1990**, 3289−3294.
(34) For example, see: (a) Haugland, R. P. *Handbook of Fluorescent Probes and Research Products*, 9th ed.; Molecular Probes, Invitrogen: Carlsbad, CA, 2002; references therein. (b) Brownlee, C. *Trends Cell Biol.* **2000**, *10*, 451−457.

Spectrometrie de Masse de l'Université Paul Sabatier et du CNRS de Toulouse. Fast-atom bombardment (FAB > 0) spectra were performed on a Nermag R10-10H spectrometer. A 9 kV xenon atom beam was used to desorb samples from the 3-nitrobenzyl alcohol matrix. Other spectra were performed on a triple quadrupole mass spectrometer (Perkin-Elmer Sciex API 365) using the electrospray ionization mode. The infusion rate was 5 μL/min. ^{1}H and ^{13}C NMR spectra were performed on Bruker AC 200, AM 250, DPX 300, and AMX 400 spectrometers. ^{1}H and ^{13}C NMR spectra were referenced to external tetramethylsilane. For 2D NMR experiments, the observation frequencies were in the range of 400.13 MHz for ^{1}H and 100.62 MHz for ^{13}C.

Electrochemical Studies. Voltammetric measurements were carried out with a homemade potentiostat[35] using the interrupt method to minimize the uncompensated resistance (iR drop). Experiments were performed at room temperature in an airtight three-electrode cell connected to a vacuum/argon line. The reference electrode consisted of a saturated calomel electrode (SCE) separated from the solution by a bridge compartment filled with the same solvent and supporting electrolyte solution. The counter electrode was a platinum wire of ca. 1 cm^2 apparent surface. The working electrode was a Pt electrode (1 mm diameter). The supporting electrolyte ^{n}Bu$_4$NBF$_4$ (99%) (Fluka electrochemical grade) was melted and dried under vacuum for 1 h. All solutions measured were 1.0×10^{-3} M in organometallic complex and 0.1 M in supporting electrolyte. The solutions were degassed by bubbling argon before the experiments. With the above reference, $E_{1/2} =$ 0.45 V vs SCE was obtained for 1 mM ferrocene (estimated experimental uncertainty of $\pm$10 mV). Cyclic voltammetry was performed in the potential range of -2 to 2 V versus SCE scanning from 0 toward 2 V/SCE for the oxidation studies (and from 0 toward -2 V/SCE for the reduction studies) at 0.1 V s^{-1} at room temperature. Before each measurement, the electrode was polished with emery paper (Norton A621). To calculate the half wave potential ($E_{1/2}$), a quasi-steady-state behavior (at the Pt working electrode, 1 mm in diameter) is obtained by the use of linear voltammetry at 5 mV s^{-1}. For cation detection experiments, concentrated acetonitrile solutions of calcium triflate (0.3$-$10 equiv) were syringed into the ferrocenyl solution under an argon atmosphere, keeping the total volume of the electrochemical mixture constant. The solution was immediately degassed and examined.

Proton NMR Titration Studies. Proton NMR titrations were typically performed as follows. A solution (500 μL) of the receptor **3** in a deuterated solvent (10^{-2} M) was added (using a microsyringe) into NMR tubes containing the appropriate quantities of solid Ca(CF$_3$SO$_3$)$_2$ salt under an inert atmosphere, while the NMR spectrum of the receptor was monitored. The samples of solid calcium were prepared by evaporating the corresponding calculated volumes of a calcium guest solution (10^{-2} M) in acetonitrile. Stability constants were evaluated from titration data using the method indicated in the main text.

Residual Error (E_r) of the Curve-Fitting Model. The residual error was calculated using the expression

$$E_r = \frac{1}{n-p-1}\sum_{i=1}^{n}(c_i - e_i)^2$$

where n is the total number of points (6×10), p is the number of unknown parameters (35 with five species, 21 when only three species are taken into account), and c_i and e_i are the calculated and experimental values of the variation of the chemical shifts, respectively. The number of unknown parameters includes the equilibrium constant for each species and their chemical shifts. This number may seem important, but it must be underlined that a simultaneous fitting on several distinct signals, 6 in our case, is much more difficult to process than a fit on a single signal.

Optical Measurements. Apparatus. UV$-$vis absorption spectra were recorded on a Hewlett-Packard 8452A diode array spectrophotometer. The absorption spectra did not vary over a period of 2 h. Cuvettes of 1 cm optical path length were used. Steady-state fluorescence work was performed on a Photon Technology International (PTI) Quanta Master 1 spectrofluorometer. All fluorescence spectra were corrected. The fluorescence quantum yield was determined relative to coumarin 6 in ethanol as the standard ($\Phi_F = 0.78$).[36] The measurements were conducted at 20°C in a thermostated cell.

Data Analysis. The absorption experimental data were processed on a HP 9000 series 710 workstation. Absorbance, A, was related to the concentration, C_i, using Beer$-$Lambert's law, $A = l\sum(\epsilon_i C_i)$, where ϵ_i is the molar absorption coefficient of the species i and l is the optical path length. The system of three equilibrium equations with three independent variables was numerically solved by an iterative method. The sum of the squares of the differences between the experimental values and those of the numerical calculation was minimized by a Powell nonlinear minimization algorithm. The method has been extensively described in a previous paper.[17]

[Fe(C$_5$H$_4$CO(CH=CH)$_2$C$_6$H$_4$NMe$_2$)$_2$] (3). A light-protected mixture of Fe(C$_5$H$_4$COMe)$_2$ (0.100 g, 0.37×10^{-3} mol), CHOCH=CHC$_6$H$_4$NMe$_2$ (0.130 g, 0.74×10^{-3}mol), and 1 equiv of NaOH was dissolved in ethanol (10 mL) and stirred for 4 h at room temperature. The mixture was evaporated to dryness. The residue was purified by column chromatography on dried silica (eluent = 5:2 petroleum ether/ethyl acetate), and the red phase was extracted with THF as the eluent (3×). After evaporation of the solvent, the product was washed with pentane (30 mL × 2) and dried to afford the desired product as a deep orange powder in a 65% yield (m = 0.140 g). ^{1}H NMR (CD$_3$CN, 293 K): δ 2.99 (s, 12H, Hp), 4.59 (br s, 4H, $^3J_{HeHf}$ = 2.0 Hz, Hf), 4.84 (br s, 4H, $^3J_{HeHf}$ = 2.0 Hz, He), 6.64 (d, 4H, $^3J_{HcHd}$ = 8.8 Hz, Hd), 6.67 (d, 2H, $^3J_{HaHb}$ = 14.8 Hz, Ha), 6.88 (dd, 2H,$^3J_{HbHg}$ = 11.2 Hz, $^3J_{HhHg}$ = 15.2 Hz, Hg), 7.02 (d, 2H, $^3J_{HhHg}$ = 15.2 Hz, Hh), 7.36 (d, 4H,$^3J_{HcHd}$ = 8.8 Hz, Hc), 7.46 (dd, 2H, $^3J_{HbHg}$ = 11.2 Hz, $^3J_{HaHb}$ = 14.8 Hz, Hb). ^{13}C {^{1}H} NMR (CD$_3$CN, 293 K): δ 39.79 (CHp), 71.27 (CHe), 73.94 (CHf), 83.40 (C$_{ipso}-$C$_5$H$_4$), 112.40 (CHd), 122.70 (CHg), 124.49 (C$_{ipso}-$C), 124.49 (CHa), 129.06 (CHc), 142.61 (CHh), 142.65 (CHb), 151.57 (C$_{ipso}-$N), 191.81 (CO). IR (CH$_3$CN): 1522, 1559, 1570, 1604, 1645 (ν_{CO}), 2873$-$2998 (ν_{CH}). ESI-MS: 585.1 [M + H] $^+$. Anal. Calcd for **3**, C$_{36}$H$_{36}$N$_2$O$_2$Fe: C, 73.97; H, 6.21; N, 4.79. Found: C, 73.72; H, 6.19; N, 4.76.

Interaction of 3 with 2 equiv of Ca(CF$_3$SO$_3$)$_2$. ^{1}H NMR(CD$_3$CN, 293 K): δ 2.99 (s, 12H, Hp), 4.80 (broad s, 4H, Hf), 5.00 (broad s, 4H, He), 6.55 (d, 4H, $^3J_{HcHd}$ = 8.8 Hz, Hd), 6.55 (d, 2H, $^3J_{HaHb}$ = 14.9 Hz, Ha), 6.78 (dd, 2H,$^3J_{HbHg}$ = 12.0 Hz, $^3J_{HgHh}$ = 14.9 Hz, Hg), 7.08 (d, 2H, $^3J_{HgHh}$ = 14.9 Hz, Hh), 7.22 (d, 4H,$^3J_{HcHd}$ = 8.8 Hz, Hc), 7.74 (dd, 2H, $^3J_{HbHg}$ = 12.0 Hz, $^3J_{HaHb}$ = 14.9 Hz, Hb). ^{13}C {^{1}H} NMR (CD$_3$CN, 293 K): δ 39.72 (CHp), 72.53 (CHe), 75.38 (CHf), 82.89 (C$_{ipso}-$C$_5$H$_4$), 112.19 (CHd), 122.03 (CHg), 122.38 (CHa), 123.95 (C$_{ipso}-$C), 129.87 (CHc), 147.10 (CHh), 148.76(CHb), 152.04 (C$_{ipso}-$N), 194.05 (CO).

[Fe(C$_5$H$_4$CO(CH=CH)$_2$C$_6$H$_4$NHMe$_2$)$_2$] [BF$_4$]$_2$ (4). HBF$_4$·Et$_2$O (2 equiv) was slowly syringed into a stirred solution of **3** (0.08 ×

(35) Cassoux, P.; Dartiguepeyron, R.; de Montauzon, D.; Tommasino, J. B.; Fabre, P. L. *Actual. Chim.* **1994**, *1*, 49−55.

(36) Reynolds, G. A.; Drexhage, K. H. *Opt. Commun.* **1975**, *13*, 222−225.

10^{-3} M) in acetonitrile (8 mL). The light-protected mixture was stirred for 1 h. After the solvent was evaporated, the product was washed with ether (30 mL) and pentane (50 mL) and dried under vacuum. A violet powder was obtained in a 68% yield. ^{1}H NMR (400 MHz, CD_3CN, 293 K): δ 3.25 (s, 12H, Hp), 4.66 (t, 4H, $^3J_{HeHf}$ = 2 Hz, Hf), 4.89 (t, 4H, $^3J_{HeHf}$ = 2 Hz, He), 6.86 (d, 2H,$^3J_{HaHb}$= 14.8 Hz, Ha), 7.11 (d, 2H, $^3J_{HgHh}$ = 15.6 Hz, Hh), 7.21 (dd, 2H, $^3J_{HbHg}$ = 10.8 Hz, $^3J_{HgHh}$ = 15.6 Hz, Hg), 7.46 (dd, 2H, $^3J_{HbHg}$ = 10.8 Hz, $^3J_{HaHb}$ = 14.8 Hz, Hb), 7.57 (d, 4H, $^3J_{HcHd}$ = 8.8 Hz, Hd) 7.72 (d, 4H, $^3J_{HcHd}$ = 8.8 Hz, Hc), 8.95 (sl, 2H, NH^+). $^{13}C\{^1H\}$ NMR (100.6 MHz, CD_3CN, 293 K): δ 47.41 (CHp), 71.53 (CHe), 74.75 (CHf), 82.57 ($C_{ipso}-C_5H_4$), 121.60 (CHd), 128.19 (CHa), 129.15 (CHc), 130.36 (CHg), 138.33 (CHh), 139.16 ($C_{ipso}-$C), 140.32 (CHb), 142.11 ($C_{ipso}-$N), 191.85 (CO). MS (ESI, CH_3-CN): 673.5 [M − BF_4^-]. Anal. Calcd for **4**, $C_{36}H_{38}N_2O_2FeB_2F_8$: C, 56.88; H, 5.04; N, 3.68. Found: C, 56.52; H, 4.95; N, 3.75.

Acknowledgment. This work was supported by the CNRS and the French Ministry of Research (doctoral fellowship to J. M.). The reviewers are acknowledged for constructive comments.

Supporting Information Available: Figure S1 showing the calculated (top) and experimental (bottom) ESI-MS spectra of the $(\mathbf{3})_3Ca^{2+}$ cation in CH_3CN, Figure S2 showing the ^{1}H NMR chemical shift variations of the mentioned protons of **3** versus the $Ca(CF_3SO_3)_2$ concentration in CD_3CN at 293 K (the calculated curves are obtained by fitting the data with the $K_1K_2K_4$ model), S3 listing the calculated values of the Δ (δ H, ppm) of **3** obtained when using the K_1-K_5 model and the $K_1K_2K_4$ model, and S4 showing the calculated concentration of each **3** adduct in the excited state using the curve-fitting model obtained when processing the UV−vis absorption data which refer to the ground state ([**3**] = 1.68×10^{-6} M in CH_3CN). This material is available free of charge via the Internet at http://pubs.acs.org.

IC060535E